Phase diagram of a binary symmetric hard-core Yukawa mixture

Elisabeth Schöll-Paschinger
Institut für Experimentalphysik, Universität Wien, Strudlhofgasse 4, A-1090 Wien, Austria
and CMS and Institut für Theoretische Physik, TU Wien, Wiedner Hauptstraße 8-10, A-1040 Wien, Austria

Dominique Levesque and Jean-Jacques Weis
Laboratoire de Physique Théorique, UMR 8627, Bâtiment 210, Université Paris-Sud,
F-91405 Orsay, France

Gerhard Kahl
CMS and Institut für Theoretische Physik, TU Wien, Wiedner Hauptstraße 8-10, A-1040 Wien, Austria

(Received 25 June 2004; accepted 15 October 2004; published online 21 December 2004)

We assess the accuracy of the self-consistent Ornstein-Zernike approximation for a binary symmetric hard-core Yukawa mixture by comparison with Monte Carlo simulations of the phase diagrams obtained for different choices of the ratio α of the unlike-to-like interactions. In particular, from the results obtained at $\alpha=0.75$ we find evidence for a critical endpoint in contrast to recent studies based on integral equation and hierarchical reference theories. The variation of the phase diagrams with range of the Yukawa potential is investigated. © *2005 American Institute of Physics.* [DOI: 10.1063/1.1829632]

I. INTRODUCTION

Symmetric binary fluid mixtures with appropriate attractive interactions can show both a liquid-vapor (LV) and a demixing transition when the relative strengths $K_{11}=K_{22}$ and K_{12} of the (attractive) interactions between particles of similar and dissimilar species are different. According to the value of $\alpha=K_{12}/K_{11}$ several distinct phase diagrams are obtained depending on where the demixing transition line (λ line) meets the LV coexistence curve.[1] If α is close to 1, the tendency for the demixing transition is small unless the temperature is low and the density high. The λ line is expected to intersect the coexistence curve at a critical end point (CEP) at a temperature well below the critical LV temperature (type I phase diagram). At lower values of α the CEP moves to higher temperatures eventually merging with the LV critical point giving rise to a tricritical point (type III). An intermediate situation can exist where the demixing transition becomes first order for a density higher than that of the LV critical density. In that case one will have a triple point, a LV critical point, and a tricritical point (type II).

These three types of phase diagrams have been found in mean field (MF) calculations and Monte Carlo (MC) simulations of a square well system with range 1.5σ (σ denotes the hard-core diameter).[1] In the simulations the type II diagram is found to occur in a rather narrow range $0.65\lesssim\alpha\lesssim0.68$ while MF theory predicts a wider range, i.e., $0.605<\alpha<0.708$.[1] Qualitatively MF and simulation results agree though there is quite a quantitative discrepancy between the values of α where one topology of the phase diagram changes to the other. This may not be so surprising as MF theory neglects fluctuations in the order parameters of the LV and demixing transitions.[1] In later work, using the hierarchical reference theory (HRT),[2] which is based on renormalization group techniques, Pini *et al.*[3] have addressed the question whether the MF picture still holds when fluctuations in the order parameters of the LV and of the demixing transitions are taken into account. They applied the HRT to a hard-core Yukawa fluid mixture (HCYFM) and found that the intermediate type II persists up to the highest value of $\alpha=0.8$ at which a reliable solution of the HRT theory could be obtained. Thus they did not find evidence for a CEP in contrast to the MF and simulation results for the square well mixture. Reference hypernetted chain (RHNC) integral equation results by Antonevych *et al.*[4] for a symmetric Lennard-Jones (LJ) mixture also arrived at the conclusion that there is no CEP.

Up to this point the different predictions for the phase behavior suggest that either the scenario of phase behavior is not generic and depends on the potential model or that the applied theories lack accuracy. In support of the latter hypothesis is a MC finite size scaling study of the demixing transition of the symmetric LJ mixture[5] which convincingly attests the existence of a CEP for $\alpha=0.7$. Similarly, integral equation results based on the self-consistent Ornstein-Zernike approximation (SCOZA),[6,18] which previously has been shown to give accurate results for the coexistence curves (including the critical region) of one component systems,[7,8] predicted all three types of phase diagram for the HCYFM model at $z\sigma=1.8$, in particular, a CEP at $\alpha=0.75$ in contrast with the HRT results of Ref. 3.

One aim of the present paper is to present MC simulation results for the HCYFM model in order to establish the accuracy of the theoretical approaches, SCOZA and HRT, restricting ourselves to the equimolar case. In addition, we investigate the change of phase diagram when the range of the Yukawa potentials increases. Interestingly, exact results are available when this range gets infinitely large[9] providing a stringent test of the SCOZA approach in this limit.

II. THEORY

A. The model

We have studied a symmetric binary HCYFM. For the parametrization of the interatomic potentials we have chosen the following form $(i,j=1,2)$:

$$\beta\Phi_{ij}(r)=\begin{cases}\infty, & r\leqslant\sigma\\ -\dfrac{K_{ij}}{r}\exp[-z(r-\sigma)], & r>\sigma,\end{cases} \tag{1}$$

where $\beta=(k_BT)^{-1}$ (k_B being the Boltzmann constant and T is the temperature) and σ is the hard-core (HC) diameter which will be used as the unit of length. z is the inverse screening length of the system. Due to the symmetry, $K_{11}=K_{22}$ and the parameter α is introduced via $K_{12}=\alpha K_{11}$. The total number density is $\rho=\rho_1+\rho_2$, where the ρ_1 and ρ_2 are the partial number densities and $x=\rho_1/\rho$ is the concentration of species 1. Reduced values $z^*=z\sigma$, $\rho^*=\rho\sigma^3$, and $T^*=\sigma/K_{11}$ will be used throughout the paper. For commodity we will drop the stars.

B. MSA and SCOZA

SCOZA is an advanced liquid state theory, which is based on a mean spherical approximation (MSA)-type closure relation to the, Ornstein-Zernike (OZ) equations; it relates the direct correlation functions $c_{ij}(r)$ and the pair distribution functions $g_{ij}(r)$, $i, j=1, 2$, to the $\Phi_{ij}(r)$ via

$$\begin{aligned} &g_{ij}(r)=0 \quad \text{for } r\leqslant 1,\\ &c_{ij}(r)=c_{\mathrm{HC};ij}(r)+K_{ij}(\rho,T,x)\Phi_{ij}(r) \quad \text{for } r>1,\end{aligned} \tag{2}$$

thereby introducing yet undetermined, state dependent functions $K_{ij}(\rho,T,x)$ which are fixed by the thermodynamic self-consistency requirement for the isothermal compressibility, calculated via the compressibility and the energy route. Taking advantage of the availability of the analytic solution of the MSA for the HCYFM with an arbitrary number of components,[10] part of the formalism can be carried out analytically.[6] It should be pointed out that at present—due to computational limitations—only a global consistency criterium can be used: here the reduced *total* isothermal compressibility $\chi_{\mathrm{red}}=\rho k_BT\chi_T$ is related to the excess (over ideal gas) internal energy per volume u by

$$\rho\frac{\partial^2 u}{\partial\rho^2}=\frac{\partial}{\partial\beta}\left(1-\frac{1}{\rho}\sum_{ij}\rho_i\rho_j\tilde{c}_{ij}(q=0)\right)=\frac{\partial}{\partial\beta}\left(\frac{1}{\chi_{\mathrm{red}}}\right), \tag{3}$$

where the tilde denotes the Fourier transforms of the $c_{ij}(r)$. So we have to reduce the number of unknown functions which was done by assuming that $K_{ij}(\rho,T,x)=K(\rho,T,x)$ for all i and j. The formalism of SCOZA (for a detailed presentation see Refs. 6 and 11) leads finally to a quasilinear parabolic partial differential equation for u

$$B(\rho,u)\frac{\partial u}{\partial\beta}=\rho\frac{\partial^2 u}{\partial\rho^2}, \tag{4}$$

which has to be solved numerically with suitable boundary and initial conditions. Details about the solution algorithm are summarized in the Appendix of Ref. 7.

Once Eq. (4) is solved, the thermodynamic properties of the system can readily be calculated. In particular, we require the pressure P and the chemical potentials μ_1 and μ_2 for the determination of the phase diagram. The coexistence equations are again solved with well-tested numerical algorithms, taking benefit of some symmetry relations in the μ's due to the symmetry in the interactions.

It should be noted that there is evidence that SCOZA results converge towards MSA results as z becomes smaller: this is reflected by the fact that for these z values $K(\rho,T,x)\sim-\beta$ (as required in the MSA) and that the degree of thermodynamic inconsistency between the compressibility and the energy route within MSA becomes smaller.

III. RESULTS

Grand canonical Monte Carlo (GCMC) simulations have been carried out for five sets of values of the parameters z and α: $z=1.8$ and $\alpha=0.65$, 0.70 and 0.75, $z=0.1$, $\alpha=0.70$ and $z=0.01$, $\alpha=0.70$. For the two lowest values $z=0.1$ and $z=0.01$ the range of the Yukawa potentials exceeds largely the size of the cubic simulation cell of volume $V=2500\sigma^3$ with periodic boundary conditions. As in the SCOZA theory the particles interact with the full Yukawa potential the long range has been taken into account in the simulations in order to make a meaningful comparison with theory. We have used the Ewald form of the Yukawa potential (cf. Appendix),[12] which includes properly the sizeable contribution of the periodic replicas of the system to the internal energy when the

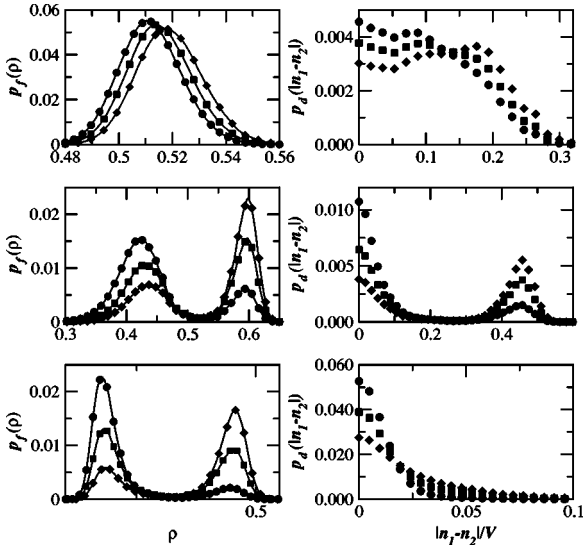

FIG. 1. From top to bottom are displayed the typical variations of p_f and p_d in the vicinity of the three different transitions occuring in the mixture. The first row corresponds to a second-order demixing transition of the mixture with $z=0.1$ and $\alpha=0.7$ located at $T=105$ and $\beta\mu=-3.14$; p_d and p_f are plotted for $\beta\mu=-3.15$ (filled circle), -3.14 (filled square), and -3.13 (filled diamond). The second row corresponds to a first-order demixing transition of the mixture with $z=1.8$ and $\alpha=0.65$ located at $T=1.03$ and $\beta\mu=-3.272$; p_d and p_f are plotted for $\beta\mu=-3.275$ (filled circle), -3.272 (filled square), and -3.270 (filled diamond). The third row corresponds to a first-order transition between undemixed phases of the mixture with $z=1.8$ and $\alpha=0.7$ located at $T=1.02$ and $\beta\mu=-3.422$, p_d, p_f are plotted for $\beta\mu=-3.425$ (filled circle), -3.422 (filled square), and -3.420 (filled diamond).

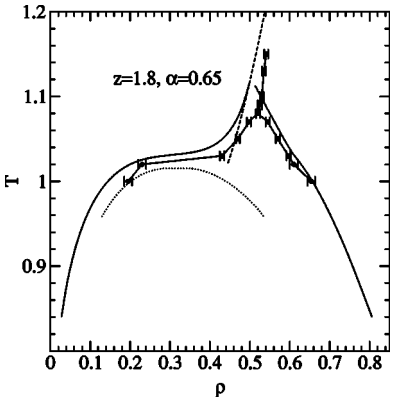

FIG. 2. Phase diagram of the HCYFM for $z=1.8$ and $\alpha=0.65$. The solid lines represent SCOZA results for first-order phase coexistence, the dashed line the λ line, and the dotted lines the metastable equimolar vapor-liquid transitions. The circles are the MC results with error bars.

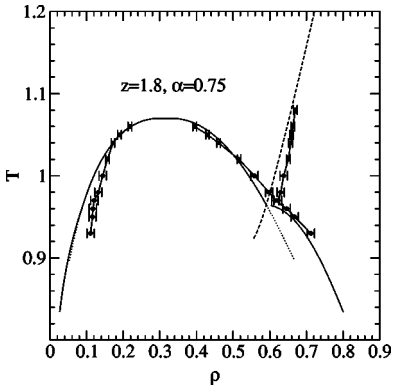

FIG. 4. Phase diagram of the HCYFM for $z=1.8$ and $\alpha=0.75$. The solid lines represent SCOZA results for first-order phase coexistence, the dashed line the λ line, and the dotted lines the metastable equimolar vapor-liquid transitions. The circles are the MC results with error bars.

Yukawa potential has a long range. The simulations have been performed with the Ewald Yukawa potential for all values of z although for our simulation box size truncation of the Yukawa potential would entail negligible effects for $z=1.8$.

All the simulations have been realized for identical chemical potentials of the two species, $\mu=\mu_1=\mu_2$, implying that, at low densities, the average numbers of the particle species $\langle n_1\rangle$ and $\langle n_2\rangle$ are equal. At a given value of temperature T and chemical potential μ, a typical simulation involved 10^8 trial MC moves (displacement, insertion, or deletion of a particle). In the bulk, equimolar, or demixed fluid phases, the relative precision on the total density $\rho=\langle n_1+n_2\rangle/V$ is $\simeq 1\%$. The location of the phase transitions is based on the determination of the joint probability of the internal energy u and numbers of particles $p(u,n_1,n_2,T,\mu)$. The latter function can be estimated directly from the simulations or computed by combining the results obtained for different, but close, values of T and μ following a reweighting procedure well documented in the literature.[13–15] The reweighted $p(u,n_1,n_2,T,\mu)$ functions were calculated from a set of simulations near the transition involving at least four MC runs of $\sim 8\times 10^8$ trial MC moves.

After summation on u, the histograms $p_f(n_1+n_2,T,\mu)$ and $p_d(|n_1-n_2|,T,\mu)$ were used to locate the phase transitions.[16] The first-order transition between the equimolar vapor and liquid is characterized by the existence of two peaks in p_f at the values of n_1+n_2 associated with the vapor and liquid densities ρ^V and ρ^L. For a given value of T, the equilibrium between these two phases is located at the value of μ_{LV} where the two peaks have equal height. The vapor and liquid phases in equilibrium are equimolar if for μ values close to μ_{LV} (below or above) a unique peak is observed in p_d at $|n_1-n_2|=0$. On the other hand, equilibrium takes place between an equimolar and demixed phase when for μ below μ_{LV}, p_d has a peak at $|n_1-n_2|=0$ and above μ_{LV} a peak at a finite value of $|n_1-n_2|$. In this case the demixing transition is a first-order transition. Typical histograms for p_f and p_d are shown in Fig. 1. For details we refer the reader to the caption.

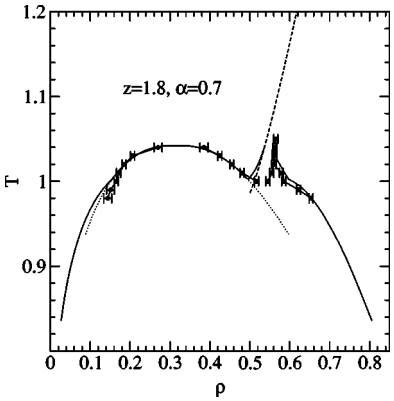

FIG. 3. Phase diagram of the HCYFM for $z=1.8$ and $\alpha=0.70$. The solid lines represent SCOZA results for first-order phase coexistence, the dashed line the λ line, and the dotted lines the metastable equimolar vapor-liquid transitions. The circles are the MC results with error bars.

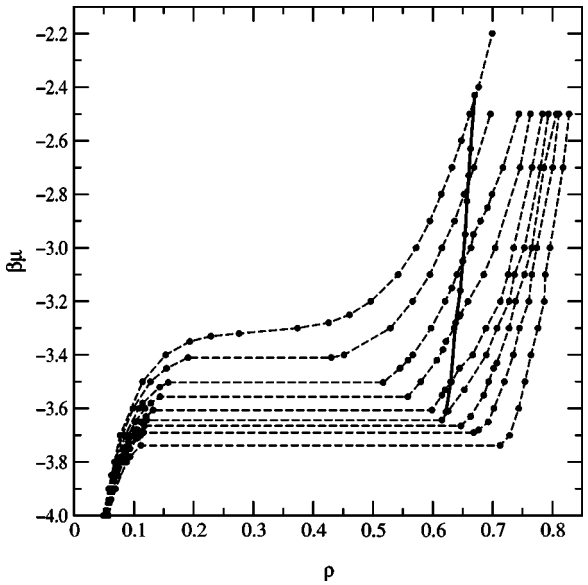

FIG. 5. Simulation results for the isotherms (dashed lines) of the HCYFM for $z=1.8$ and $\alpha=0.75$; from top to bottom: $T=1.08$, 1.05, 1.02, 1.00, 0.98, 0.97, 0.96, 0.95, and 0.93. Full line—λ line.

TABLE I. Coexistence densities as a function of α and T for $z=1.8$; ρ^V and ρ^L are the equimolar vapor and liquid coexistence densities; ρ_d and ρ_d^L the coexistence densities at the demixing transition; $\Delta\rho$ is the error on the densities; $\beta\mu_{\mathrm{LV}}$ is the chemical potential (times β) at the LV transition; $\beta\mu_\lambda$ is the chemical potential (times β) at either the λ line, the equimolar-demixed liquid transition or the equimolar vapor-demixed liquid transition.

T	ρ^V	ρ^L	ρ_λ	ρ_d	ρ_d^L	$\Delta\rho$	$\beta\mu_{\mathrm{LV}}$	$\beta\mu_\lambda$
				$\alpha=0.65$				
1.15			0.541			0.005		−2.48
1.13[a]			0.535			0.005		−2.61
1.10			0.530			0.005		−2.80
1.09[a]			0.525			0.005		−2.87
1.08[a]			0.520			0.005		−2.943
1.07	0.498				0.545	0.005		−3.008
1.05	0.470				0.570	0.005		−3.142
1.03	0.430				0.597	0.005		−3.272
1.02[a]	0.230				0.610	0.01		−3.337
1.00	0.195				0.654	0.01		−3.403
				$\alpha=0.70$				
1.05			0.565			0.005		−3.080
1.04[a]	0.270	0.385	0.563			0.005	−3.352	−3.165
1.03[a]	0.206	0.425	0.562			0.005	−3.386	−3.225
1.02	0.185	0.455	0.560			0.005	−3.422	−3.305
1.01	0.171	0.480		0.555	0.579	0.005	−3.456	−3.385
1.00	0.165	0.517		0.545	0.585	0.005	−3.483	−3.464
0.99	0.151				0.622	0.01		−3.517
0.98	0.144				0.653	0.01		−3.542
				$\alpha=0.75$				
1.08			0.670			0.005		−2.430
1.06[a]	0.218	0.395	0.663			0.005	−3.376	−2.630
1.05	0.190	0.430	0.660			0.005	−3.410	−2.730
1.04[a]	0.172	0.460	0.657			0.005	−3.443	−2.825
1.02	0.157	0.516	0.651			0.005	−3.503	−3.050
1.00	0.144	0.558	0.638			0.01	−3.556	−3.280
0.98	0.132	0.598	0.630			0.01	−3.606	−3.500
0.97	0.121	0.615	0.622			0.01	−3.643	−3.612
0.96	0.117				0.646	0.01		−3.665
0.95	0.116				0.668	0.01		−3.690
0.93	0.111				0.712	0.01		−3.738

[a]Reweighted isotherms.

At high temperatures, the demixing transition is a second-order transition (cf. Introduction). For a given value of T and increasing values of μ, it is characterized first by the broadening of the peak of p_d at $|n_1-n_2|=0$. The value μ_λ of μ at which the peak reaches its maximum width gives the location of the λ line at density ρ_λ. Above μ_λ the value of $p_d(0,T,\mu)$ decreases and a peak located at values of $|n_1-n_2|\neq 0$ gives the demixing rate $|n_1-n_2|/(n_1+n_2)$ of the demixed phase. This variation of p_d does not correspond to any qualitative change of p_f which presents a narrow unique peak at values of $\rho=\langle n_1+n_2\rangle/V$ increasing monotonically with μ.

The above procedure for locating the first-order transitions applies easily when, at the phase equilibrium, the difference between the vapor density ρ^V and the equimolar (or demixed) liquid density ρ^L (or ρ_d^L) or between the coexisting liquid densities at the demixing transition, ρ_d and ρ_d^L, is smaller than 0.3 (here the subscript "d" denotes coexistence densities of the demixing transition). For these density differences, several transitions between the low and high density phases occur in a MC run, giving an adequate sampling of $p(u,n_1,n_2,T,\mu)$, in particular, of the relative heights of the peaks associated with the two phases. At low temperature, the density gap between the vapor and demixed liquid is large and cannot be crossed during a MC run without biased sampling, for instance, multicanonical sampling.[17] Such a sampling has not been used in this work and the vapor-demixed liquid transitions at low temperatures have been localized by looking for a value of μ such that above and below this value the vapor and liquid phases are, respectively, unstable. The uncertainty on the equilibrium densities determined from the analysis of $p(u,n_1,n_2,T,\mu)$ is estimated to be ± 0.005; at low temperatures, where this analysis could not be performed the error is estimated to be ± 0.01.

The phase diagrams for $z=1.8$ are shown in Figs. 2–4 where α varies from 0.65 to 0.75. A set of isotherms for $\alpha=0.75$ is plotted in Fig. 5. The coexistence densities of the various phases and the densities along the λ line are summarized in Tables I–III for the different isotherms considered in the simulations.

The phase diagram at $\alpha=0.65$ (cf. Fig. 2) is clearly of type III. There is no LV critical point but a tricritical point at $T_{\mathrm{tr}}\approx 1.075$ and $\rho_{\mathrm{tr}}\approx 0.517$. Upon increasing α to 0.7, a LV critical point emerges which for $\alpha=0.7$ has critical parameters $T_c\approx 1.045$ and $\rho_c\approx 0.305$. The tricritical point has a temperature $T_{\mathrm{tr}}\approx 1.02$, i.e., lower than the critical temperature and a density $\rho_{\mathrm{tr}}\approx 0.56$ (type II phase diagram). At

TABLE II. Same as Table I but for $\alpha=0.7$ and $z=0.1$.

T	ρ^V	ρ^L	ρ_λ	ρ_d	ρ_d^L	$\Delta\rho$	$\beta\mu_{\mathrm{LV}}$	$\beta\mu_\lambda$
110			0.529			0.005		−2.79
107[a]			0.519			0.005		−3.00
105	0.195	0.310	0.515			0.005	−3.510	−3.14
104[a]	0.165	0.336				0.005	−3.538	
103[a]	0.151	0.360	0.504			0.005	−3.566	−3.30
102	0.143	0.380	0.502			0.005	−3.595	−3.371
100	0.127	0.421	0.497			0.005	−3.648	−3.512
99			0.493			0.005		−3.590
98	0.115	0.464	0.490			0.01	−3.698	−3.665
97	0.102	0.480		0.480	0.515	0.01	−3.738	−3.738
96	0.107				0.565	0.01		−3.745
95	0.106				0.593	0.01		−3.760
90	0.092				0.675	0.01		−3.863

[a]Reweighted isotherms.

$\alpha=0.75$ the λ line intersects the LV coexistence curve at a critical end point $T_{\mathrm{cep}}\approx 0.965$, $\rho_{\mathrm{cep}}\approx 0.617$ (type I phase diagram). The critical temperature $T_c\approx 1.07$ is slightly higher than for $\alpha=0.7$ but the critical density $\rho_c\approx 0.305$ is unchanged within statistical error.

The sequence of phase diagrams obtained by SCOZA for $z=1.8$ is similar to that found in the simulations. In fact, the phase diagrams obtained with SCOZA and simulations compare quite favorably. As seen from Figs. 2–4 agreement is excellent for the vapor-equimolar liquid transition. The demixing transition occurs in the GCMC results for densities systematically larger than in SCOZA theory, the difference being of the order of 2%–5%. Similar differences occur for the equilibrium densities between the vapor and the demixed liquid. The temperatures of the tricritical and critical end point are also in good agreement, the discrepancy being of the order of the uncertainty, i.e., 0.5%–1%, on the temperatures determined from the simulation data. For a quantitative comparison of the theoretical results and simulation data we refer to Table IV.

In Figs. 6 and 7 and Tables II and III we show the phase diagrams for $\alpha=0.7$ when the range of the Yukawa potential increases. At $z=0.1$ a narrow temperature range between $T=96$ and 98 is found in simulation where equimolar and demixed liquids coexist with $T_{\mathrm{tr}}\approx 97.5$ and $\rho_{\mathrm{tr}}\approx 0.49$; SCOZA predicts $T_{\mathrm{tr}}\approx 101$ and $\rho_{\mathrm{tr}}\approx 0.48$. As becomes visible from Fig. 6 both simulations and SCOZA predict a kink at the triple point of the coexistence curve. Upon further increasing the range of the potential to $z=0.01$ we recover a type II phase diagram with coexistence between an equimolar and a demixed liquid in the temperature range 8850–9100 with a tricritical point at $T_{\mathrm{tr}}\approx 9100$ and $\rho_{\mathrm{tr}}\approx 0.479$, in good agreement with SCOZA results $T_{\mathrm{tr}}\approx 9220$ and $\rho_{\mathrm{tr}}\approx 0.48$. Similar as for $z=1.8$ we note that the MC vapor-liquid transition curve is very well reproduced by the SCOZA theory.

Finally, we point out that for the GCMC simulations the temperature range for the existence of the first-order demixing transition is non-monotonic as z decreases towards zero, as shown by the variation of the ratio $(T_{\mathrm{tr}}-T_{\mathrm{trp}})/T_{\mathrm{trp}}$ (cf. Table IV), which is, respectively, equal to 0.025 ± 0.005 ($z=1.8$, $\alpha=0.7$), 0.005 ± 0.005 ($z=0.1$, $\alpha=0.7$), and 0.017

TABLE III. Same as Table I but for $\alpha=0.7$ and $z=0.01$.

T	ρ^V	ρ^L	ρ_λ	ρ_d	ρ_d^L	$\Delta\rho$	$\beta\mu_{\mathrm{LV}}$	$\beta\mu_\lambda$
10 000			0.530			0.005		−2.83
9 800[a]			0.522			0.005		−2.99
9 700[a]			0.516			0.005		−3.06
9 600[a]	0.185	0.315				0.005	−3.519	
9 500	0.160	0.345	0.508			0.005	−3.549	−3.23
9 400[a]			0.502			0.005		−3.32
9 300	0.135	0.390	0.495			0.005	−3.615	−3.41
9 200[a]			0.489			0.005		−3.49
9 400	0.122	0.430	0.484			0.005	−3.668	−3.568
9 000	0.115	0.461		0.480	0.510	0.01	−3.690	−3.655
8 900	0.115				0.534	0.01		−3.712
8 800	0.110				0.565	0.01		−3.739

[a]Reweighted isotherms.

TABLE IV. SCOZA values for the temperatures and densities of critical, tricritical, and critical end points obtained for the five HCYFM systems investigated. T_{trp} denotes the triple point temperature; for comparison, GCMC results are given in brackets with a typical uncertainty of 0.2%–0.3%.

$z=1.8$	$\alpha=0.65$	Type III	$T_{\mathrm{tr}}\approx 1.12$ (1.075) $\rho_{\mathrm{tr}}\approx 0.50$ (0.517)
$z=1.8$	$\alpha=0.70$	Type II	$T_c\approx 1.04$ (1.045) $\rho_c\approx 0.315$ (0.305) $T_{\mathrm{tr}}\approx 1.05$ (1.02) $\rho_{\mathrm{tr}}\approx 0.54$ (0.56) $T_{\mathrm{trp}}\approx 1.002$ (0.995)
$z=1.8$	$\alpha=0.75$	Type I	$T_{\mathrm{cep}}\approx 0.97$ (0.965) $\rho_{\mathrm{cep}}\approx 0.59$ (0.617) $T_c\approx 1.07$ (1.07) $\rho_c\approx 0.315$ (0.305)
$z=0.1$	$\alpha=0.70$	Type II	$T_c\approx 106.1$ (106.0) $\rho_c\approx 0.25$ (0.25) $T_{\mathrm{tr}}\approx 101.0$ (97.5) $\rho_{\mathrm{tr}}\approx 0.48$ (0.49) $T_{\mathrm{trp}}\approx 96.9$ (97.0)
$z=0.01$	$\alpha=0.70$	Type II	$T_c\approx 9717$ (9750) $\rho_c\approx 0.25$ (0.25) $T_{\mathrm{tr}}\approx 9220$ (9100) $\rho_{\mathrm{tr}}\approx 0.48$ (0.479) $T_{\mathrm{trp}}\approx 8870$ (8950)

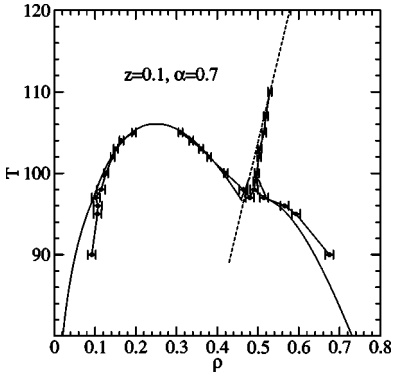

FIG. 6. Phase diagram of the HCYFM for $z=0.1$ and $\alpha=0.70$. The solid lines represent SCOZA results for first-order phase coexistence, the dashed line the λ line. The circles are the MC results with error bars.

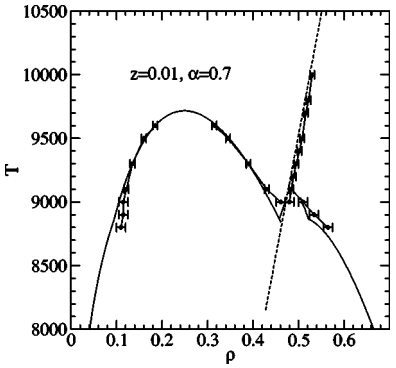

FIG. 7. Phase diagram of the HCYFM for $z=0.01$ and $\alpha=0.70$. The solid lines represent SCOZA results for first-order phase coexistence, the dashed line the λ line. The circles are the MC results with error bars.

± 0.005 ($z=0.01$, $\alpha=0.7$). However, in SCOZA this sequence was found to be monotonic: 0.048 ($z=1.8$, $\alpha=0.7$), 0.042 ($z=0.1$, $\alpha=0.7$), and 0.040 ($z=0.01$, $\alpha=0.7$).

IV. CONCLUSIONS

One of the aims of this paper was to resolve the discrepancy between predictions of two different theoretical approaches, SCOZA and HRT, for the phase diagrams of the HCYFM at values of $\alpha \gtrsim 0.73$. While SCOZA provides a clear prediction of a CEP (type I), no such evidence was found in the HRT calculations;[3] rather a type II behavior with a tricritical point is predicted up to $\alpha=0.8$, the highest value at which solution of the HRT equations could be obtained.[3] The good agreement between SCOZA and the present MC results pleads in favor of a type I phase diagram for $\alpha \gtrsim 0.73$. We note here that the range of existence of the type II phase diagram of the HCYFM, given by the simulation and SCOZA, is shifted to somewhat higher values of α compared to the square-well binary fluid mixture where the range of this phase diagram type (cf. Introduction) is $0.65<\alpha<0.68$.[1] The similarity of phase diagrams found for binary fluid mixtures of square well,[1] hard-core Yukawa,[6] LJ systems[5] as well as for classical spin systems,[19] dipolar models,[20,21] or living polymers[22] suggests a generic behavior for a wide class of potential models.[1]

The precision of SCOZA even improves when the range of the Yukawa potential increases. In the limit of infinite range an exact result can be derived for $z=0$ (Ref. 9) exhibiting a rigorous scaling of the transition temperatures as $1/z^2$, which for finite z is approximately reproduced by the MC and SCOZA results.

ACKNOWLEDGMENTS

This work was supported by the Österreichische Forschungsfond under Project Nos. P-14371-TPH and P15758-TPH and a grant through the Program d'Actions Intégrées AMADEUS under Project Nos. 06648PB and 7/2004. E.S.P. and G.K. acknowledge the warm hospitality at the Laboratoire de Physique Théorique (Université Paris-Sud, Orsay) where part of this work was done. Computing time was granted by Institut du Développement et des Ressources en Informatique Scientifique (IDRIS), Orsay. Discussions with Jean-Michel Caillol were appreciated.

APPENDIX: EWALD SUMMATION

Using an Ewald summation method the energy of the (one component) Yukawa system

$$U=\frac{1}{2}\Gamma\sum_{i,j;i\neq j}\frac{\exp(-zr_{ij})}{r_{ij}} \tag{A1}$$

can be written[12]

$$\begin{aligned}U_{(i\neq j)}=&\frac{1}{2}\Gamma\sum_{i,j;i\neq j}\sum_{n}\left\{\operatorname{erfc}\left(\gamma|\mathbf{r}_{ij}+\mathbf{H}\cdot\mathbf{n}|+\frac{z}{2\gamma}\right)\right.\\&\times\exp(z|\mathbf{r}_{ij}+\mathbf{H}\cdot\mathbf{n}|)+\operatorname{erfc}\left(\gamma|\mathbf{r}_{ij}+\mathbf{H}\cdot\mathbf{n}|-\frac{z}{2\gamma}\right)\\&\left.\times\exp(-z|\mathbf{r}_{ij}+\mathbf{H}\cdot\mathbf{n}|)\right\}\frac{1}{2|\mathbf{r}_{ij}+\mathbf{H}\cdot\mathbf{n}|}\\&+\frac{1}{2}\Gamma\sum_{i,j;i\neq j}\frac{4\pi}{V}\sum_{\mathbf{G}}\frac{\exp[-(\mathbf{G}^2+z^2)/4\gamma^2]}{\mathbf{G}^2+z^2}\\&\times\exp(i\mathbf{G}\cdot\mathbf{r}_{ij});\end{aligned} \tag{A2}$$

for the self-term we obtain

$$\begin{aligned}U_{\text{self}}=&\frac{1}{2}\Gamma N\left\{\sum_{n\neq 0}\left\{\operatorname{erfc}\left(\gamma|\mathbf{H}\cdot\mathbf{n}|+\frac{z}{2\gamma}\right)\exp(z|\mathbf{H}\cdot\mathbf{n}|)\right.\right.\\&\left.+\operatorname{erfc}\left(\gamma|\mathbf{H}\cdot\mathbf{n}|-\frac{z}{2\gamma}\right)\exp(-z|\mathbf{H}\cdot\mathbf{n}|)\right\}\frac{1}{2|\mathbf{H}\cdot\mathbf{n}|}\\&+\frac{4\pi}{V}\sum_{\mathbf{G}}\frac{\exp[-(\mathbf{G}^2+z^2)/4\gamma^2]}{\mathbf{G}^2+z^2}-\frac{2\gamma}{\sqrt{\pi}}\\&\left.\times\exp(-z^2/4\gamma^2)+z\operatorname{erfc}\left(\frac{z}{2\gamma}\right)\right\}.\end{aligned} \tag{A3}$$

In the above expressions $\mathbf{H}$ is a 3×3 matrix whose columns are the Cartesian components of the three vectors describing the parallelepipedic box $\{\mathbf{a},\mathbf{b},\mathbf{c}\}$ which for the case of a cubic simulation cell ($L_x=L_y=L_z$) becomes proportional to the unit matrix. The volume is $V=\det\mathbf{H}$. Further, $\mathbf{k}=2\pi({}^{t}\mathbf{H})^{-1}\mathbf{n}$ denotes all possible reciprocal vectors compatible with the box geometry; $({}^{t}\mathbf{H})^{-1}$ is the inverse of the transposed matrix $\mathbf{H}$, defined above, and $\mathbf{n}=(n_1,n_2,n_3)$ with n_i integers. The parameter γ controls the rate of convergence of the sums in direct and reciprocal space. It can be noted that in Eqs. (A2) and (A3) the sums in reciprocal space include the $\mathbf{G}=0$ term. In the limit $z\to 0$ a compensating background term $(-4\pi/\gamma^2V)$ has to be added to the sum to prevent divergence of these terms.[12] The above expressions can be generalized easily to the binary case.

[1] N. B. Wilding, F. Schmid, and P. Nielaba, Phys. Rev. E **58**, 2201 (1998).
[2] A. Parola and L. Reatto, Adv. Phys. **44**, 211 (1995); A. Reiner and G. Kahl, Phys. Rev. E **65**, 046701 (2002); J. Chem. Phys. **117**, 4925 (2002).
[3] D. Pini, M. Tau, A. Parola, and L. Reatto, Phys. Rev. E **67**, 046116 (2003).

[4] O. Antonevych, F. Forstmann, and E. Diaz-Herrera, Phys. Rev. E **65**, 061504 (2002).
[5] N. B. Wilding, Phys. Rev. E **67**, 052503 (2003).
[6] E. Schöll-Paschinger and G. Kahl, J. Chem. Phys. **118**, 7414 (2003).
[7] D. Pini, G. Stell, and R. Dickman, Phys. Rev. E **57**, 2862 (1998).
[8] D. Pini, G. Stell, and N. B. Wilding, Mol. Phys. **95**, 483 (1998).
[9] J.-M. Caillol (unpublished).
[10] L. Blum and J. S. Høye, J. Stat. Phys. **19**, 317 (1978); E. Arrieta, C. Jedrzejek, and K. N. Marsh, J. Chem. Phys. **95**, 6806 (1991).
[11] E. Schöll-Paschinger, Ph.D. thesis, Technische Universität Wien, 2002; thesis available from the homepage: http://tph.tuwien.ac.at/~paschinger/ and download ''Ph.D.''
[12] G. Salin and J.-M. Caillol, J. Chem. Phys. **113**, 10459 (2000).
[13] A. M. Ferrenberg and R. H. Swendsen, Phys. Rev. Lett. **63**, 1195 (1989).
[14] H.-P. Deutsch, J. Stat. Phys. **67**, 1039 (1992).
[15] M. Alvarez, D. Levesque, and J.-J. Weis, Phys. Rev. E **60**, 5495 (1999).
[16] E. Schöll-Paschinger, D. Levesque, J.-J. Weis, and G. Kahl, Phys. Rev. E **64**, 011502 (2001).
[17] B. Berg and T. Neuhaus, Phys. Rev. Lett. **68**, 9 (1992).
[18] E. Schöll-Paschinger, E. Gutlederer, and G. Kahl, J. Mol. Liq. **112**, 5 (2004).
[19] J.-J. Weis, M. J. P. Nijmeijer, J. M. Tavares, and M. M. Telo da Gama, Phys. Rev. E **55**, 436 (1997); J. M. Tavares, M. M. Telo da Gama, P. I. C. Teixeira, J.-J. Weis, and M. J. P. Nijmeijer, *ibid.* **52**, 1915 (1995).
[20] H. Zhang and M. Widom, Phys. Rev. E **49**, R3591 (1994).
[21] B. Groh and S. Dietrich, Phys. Rev. E **50**, 3814 (1994); Phys. Rev. Lett. **72**, 2422 (1994); **74**, 2617 (1997).
[22] S. J. Kennedy and J. C. Wheeler, J. Chem. Phys. **78**, 953 (1983).